

Development of a novel power processing unit for Hall thrusters

IEPC-2013-248

*Presented at the 33rd International Electric Propulsion Conference,
The George Washington University • Washington, D.C. • USA
October 6 – 10, 2013*

Naoji Yamamoto¹

Kyushu University, Kasuga, Fukuoka, 816-8580, Japan

Haruki Takegahara², Junichiro Aoyagi³ and Kyoichi Kuriki⁴
Tokyo Metropolitan University, 191-0065, Tokyo, Japan

Taichiro Tamida⁵

Mitsubishi Electric Corporation, Hyogo, 661-8661, Japan

and

Hiroyuki Osuga⁶

Mitsubishi Electric Corporation, Kamakura, 247-8520, Japan

Abstract: We have been developing a new concept PPU, which has the advantages of smaller size and lighter weight than conventional one. The thrust performance of magnetic layer type Hall thruster developed at Kyushu University with this new PPU was investigated and it showed a good performance compared to conventional power supplies. The thrust to power ratio is improved to 58 mN/kW at discharge voltage of 150 V and anode xenon mass flow rate of 1.0 mg/s.

I. Introduction

High power electric propulsion systems will be in the practical application phase in the near future. They will be used as the main propulsion system of the cargo for manned mission to Mars^{1,2}, as well as for the construction of heavy space structures like a space solar power system^{3,4}. There are many candidates for high power electric propulsions and Hall thrusters^{5,6} are one of the candidates, since they offer an attractive combination of high thrust efficiency, exceeding 50%, with a specific impulse range of 1,000-3,000 s, a higher ion beam density than ion thrusters and a larger expected total impulse. In addition, in the near future, the Hall thrusters will be a main propulsion system for super low orbit satellites and will be required to be designed as small as possible because of the installation limitations on a rocket payload⁷. These limitations require a power processing unit (PPU) size to be smaller and weight to be lighter with low power consumption operation and quick response of plasma ignition for drag compensation. Space Sub-systems Electrical Engineering Department

¹ Associate Professor, Department of Advanced Energy Engineering Science, yamamoto@aes.kyushu-u.ac.jp

² Professor, Department of Aerospace Engineering, hal@astak3.sd.tmu.ac.jp

³ Assistant Professor, Department of Aerospace Engineering, j-aoyagi@astak3.sd.tmu.ac.jp

⁴ Visiting Professor, Department of Aerospace Engineering, kuriki@astak3.sd.tmu.ac.jp

⁵ Senior Researcher, Advanced Technology R&D Center, Tamida.Taichiro@aj.MitsubishiElectric.co.jp.

⁶ Senior engineer, Space Sub-systems Electrical Engineering Department, Osuga.Hiroyuki@bx.MitsubishiElectric.co.jp

For the small and lightweight PPU, we adopt a new PPU concept; the PPU provides no more than constant voltage DC power, it provides controlled but coordinated power with the Hall thrusters, for the Hall thruster naturally works. In the Hall thrusters, discharge current naturally oscillates due to the various instabilities, and the largest of all is prey-predator oscillation (ionization oscillation)⁸⁻¹⁴. “Stability” should be re-defined not as “suppress oscillation” but as “keep discharge” and the PPU allows natured discharge oscillation as far as the discharge keeps. The coordinated PPU provides power in accordance with the time-fluctuated impedance of the Hall thrusters. That is, it works as a constant voltage source for keeping discharge when the discharge current is small and it works as a constant current source when the large pulsed current flows. The aim of this study is to demonstrate the coordinated PPU and to show the superiority of this.

II. Experimental setup

Figure 1(a) shows a cross-section of the 1 kW class magnetic layer type Hall thruster used in the current experiments. The inner and outer diameters of the acceleration channel are 50 mm and 70 mm respectively. The acceleration channel is made of boron nitride. The Anode is set at 30 mm upstream of the thruster exit. An inner solenoid coil and four outer solenoid coils create a predominantly radial magnetic field in the acceleration channel, as shown in Fig. 1(b). The magnetic flux density is varied by changing the coil current. The magnetic field distribution along the channel median is shown in Fig. 2(a) and the calculated magnetic field lines is shown in Fig. 2(b) (each coil current is 1 A, calculated using Magnum3.0, Field Precision LLC.). The origin of Fig.2(a) is the exit of the acceleration channel, and the radial magnetic flux density has peak at $z = -1$ mm. Magnetic flux density is higher on the inner wall and decreases with radius, since the magnetic flux between the poles is conserved.

99.999% High-purity xenon gas was used as the propellant with thermal mass flow controllers. A hollow cathode (Veeco Instruments Inc. HC252) is used as the electron source. Tests are conducted in a vacuum chamber of 1.0 m diameter by 1.2 m length. The pumping system includes a rotary pump and a turbo molecular pump (air pumping speed is 2050 l/s) and cryogenic pump (air pumping speed is 2300 l/s). The chamber baseline pressure is below 1×10^{-3} Pa. The background pressure was maintained below 1×10^{-2} Pa at xenon mass flow rate of 1.2 mg/s (anode 1.0 mg/s and cathode 0.2 mg/s).

Pendulum type thrust stand is used for the thrust measurement. To reduce the influence of thermal drift, low thermal expansion carbon/carbon composite ($0.08 \times 10^{-6} / \text{K}$) is used as a leg component. Thrust stand calibration is conducted with a set of two known weights in a pulley system assembly. The overall uncertainty in thrust is conservatively estimated at $\pm 5\%$. An ion collector (diameter of 2 mm) is set at 300 mm downstream of the thruster for the measurement of the ion beam current from the thruster.

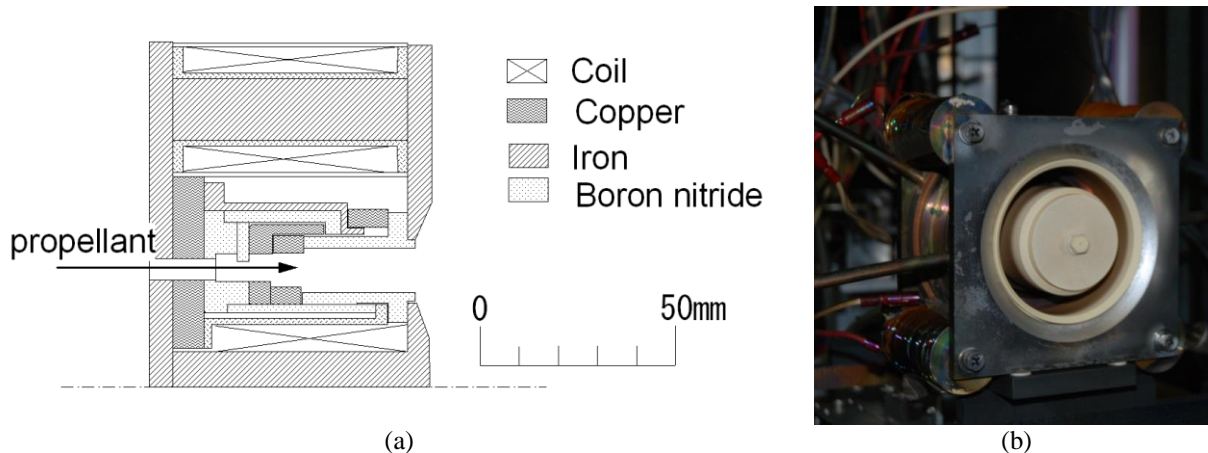


Figure 1. Magnetic layer type Hall thruster developed at Kyushu University. (a) Cross section (b)photo

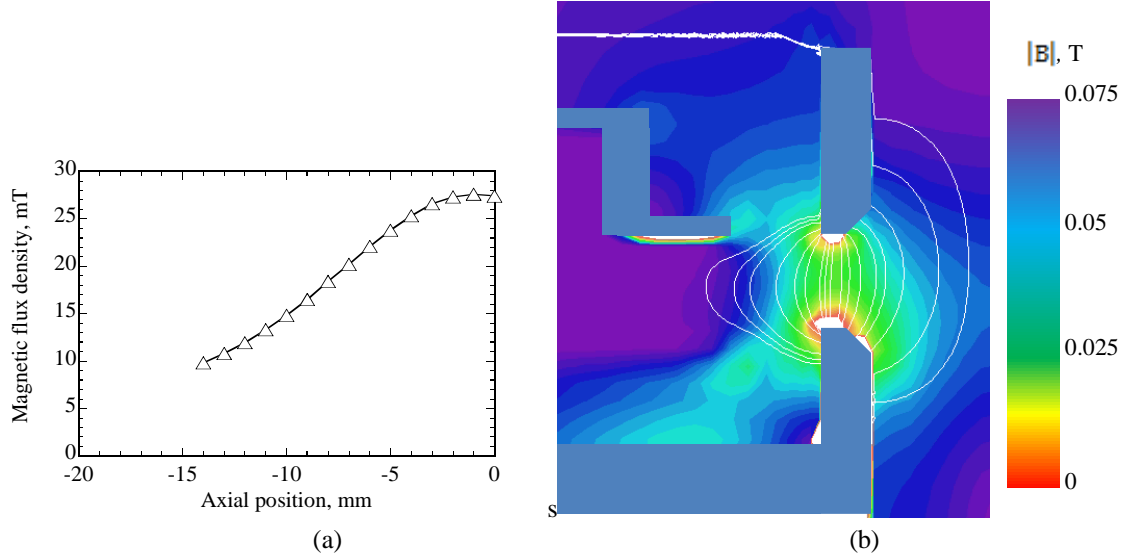


Figure 2. Magnetic field configuration of the Hall thruster developed at Kyushu University. (a) Radial magnetic flux density profile (outer coil current = 1 A, inner coil current= 1A, $r=30$ mm) (b) Calculated magnetic field lines (Calculated using Magnum3.0, Field Precision LLC.)

III. Results and discussion

In order to evaluate the performance of Hall thrusters, specific impulse, I_{sp} , and thrust efficiency, η_t are defined as,

$$I_{sp} = \frac{F}{\dot{m} g} \quad (1)$$

$$\eta_t = \frac{F^2}{2\dot{m} \int_0^T V_d I_d dt / T}$$

where, F is the thrust, \dot{m} is the anode mass flow rate, g is an acceleration of gravity, V_d is the discharge voltage, I_d is the discharge current and T is a constant time which longer than the oscillation period.

A. Rectangular Pulse Train Superposition on Constant Voltage

The characteristics of the Hall thruster with varying discharge voltage were investigated, as an initial study. We applied rectangular pulse train superposition on constant voltage to the Hall thruster using the electric circuit, as shown in Fig. 3. Figure 4 shows the discharge current trace and the ion beam current at mass flow rate of 1.36 mg/s, inner coil current of 0.5 A, outer coil current of 2 A, rectangle pulse voltage (V_p) of 50V and base discharge voltage (V_0) of 200V, chopping frequency of 22 kHz, duty ratio of 25%. The increase in the discharge current coordinates with the increase in the discharge voltage; the discharge current oscillates at frequency of 22 kHz, it is larger frequency than the nature frequency (20 kHz) of ionization oscillation (prey-predator oscillation) at constant discharge voltage of 250 V. The ion beam current also oscillates at frequency of 22 kHz, this shows that the ionization occurred at frequency of 22 kHz. That is, the PPU coordinates with the thruster under the PPU control.

Now we showed that the PPU can control the thruster, we investigate the dependency of the chopping frequency on the phase difference between the discharge current and the discharge voltage. Figure 5 shows the discharge current and discharge voltage trace for three chopping frequencies, 15, 17 and 20 kHz. The dependency of chopping frequency on the phase difference is almost the same as that on LC circuits. That is, the thruster works as a capacitive load when the frequency is low, and the phase of current leads. The thruster works as an inductive load when the frequency is high and the phase of current lags. These results show that the thruster can be treated as LC circuit.

Next we focus on the dependency of the chopping frequency on the thrust performance. Figure 6 shows the relation between the thrust/power consumption and the chopping frequency. The thrust and the power consumption

are low at 15 kHz, in which the current leads. At 17 kHz, where the phase difference is almost zero between the discharge voltage and the discharge current, the thrust and the power consumption is the largest among three frequencies. The thrust efficiency becomes minimum due to the largest power consumption. At 20 kHz, the phase lags and electricity consumption is lower than that at 17 kHz, but the thrust is almost the same as that at 17 kHz. The thrust performance of 20 kHz is the best among three frequencies. These results suggest that the phase current lag should have the thrust performance improved. We also investigate the minimum base voltage. We can keep discharge with the base discharge voltage of 100 V. However, at V_0 of 50 V, there is periods that the discharge current is almost zero. At this condition, the thrust decreases and the operation ceases after a couple of minutes. There is a threshold base voltage for stable operation, and in this case, it is 100 V.

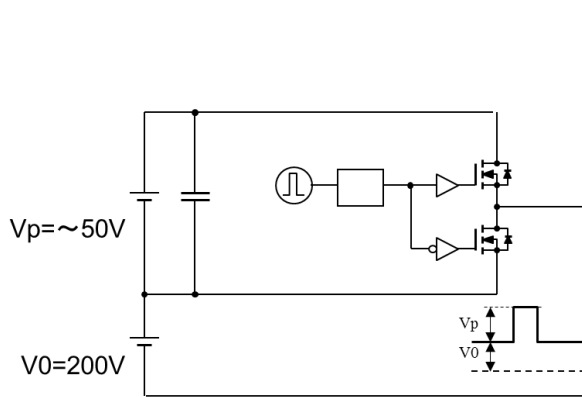


Figure 3. Rectangular Pulse Train circuit.

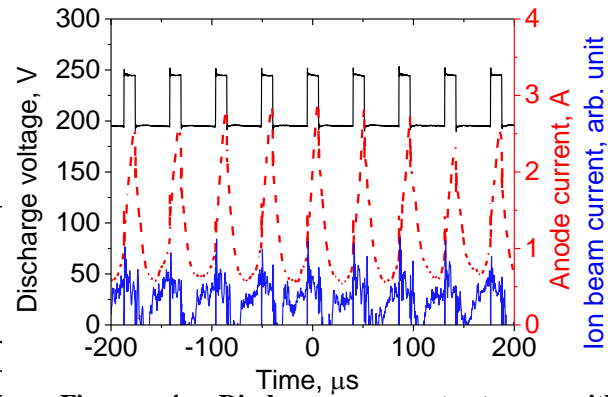


Figure 4. Discharge current trace with rectangular pulse train voltage.

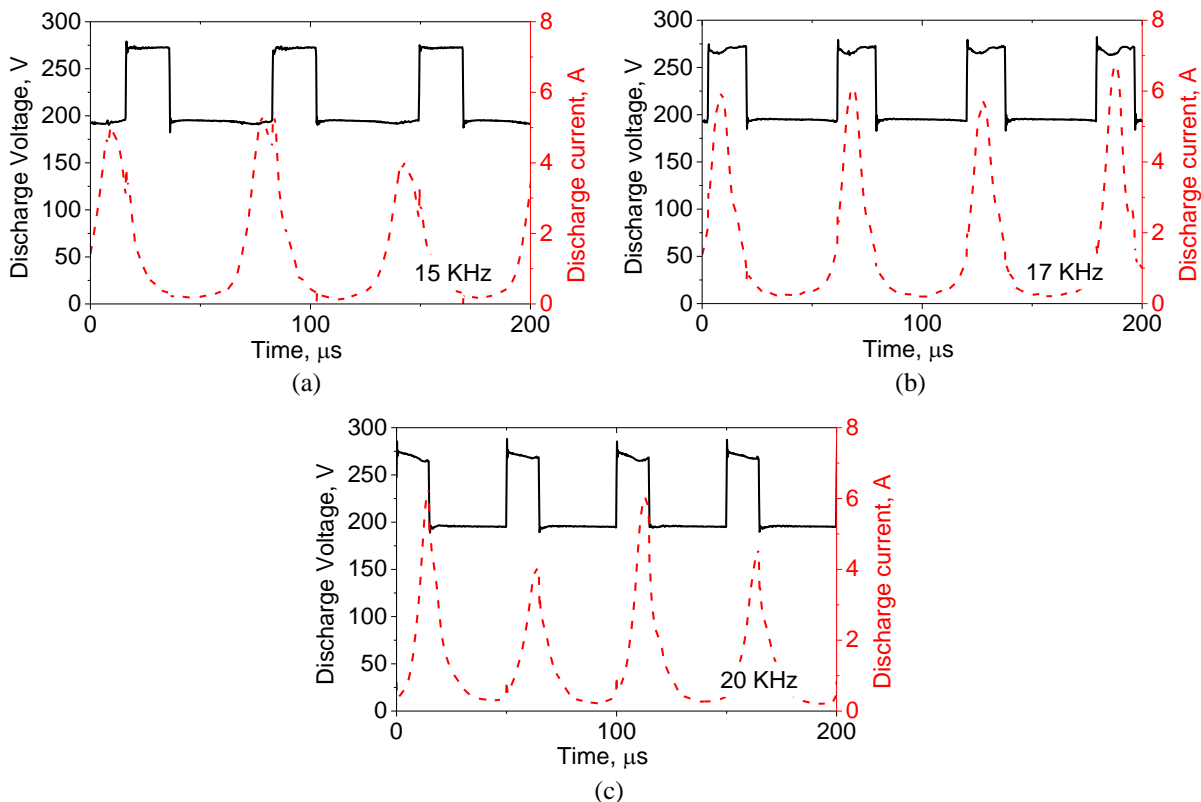


Figure 5. Current trace for three chopping frequencies. (a)15 kHz, (b)17 kHz, (c)20 kHz

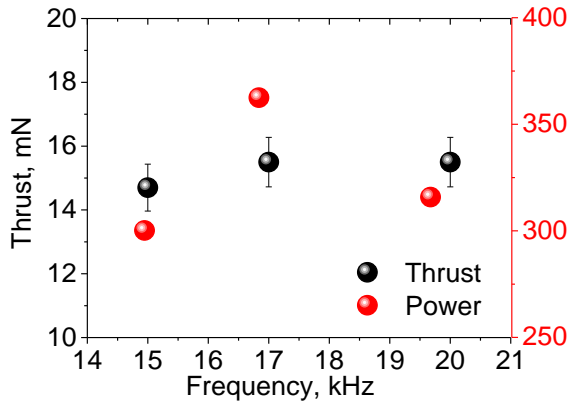


Figure 6. Thrust performance and electricity consumption.

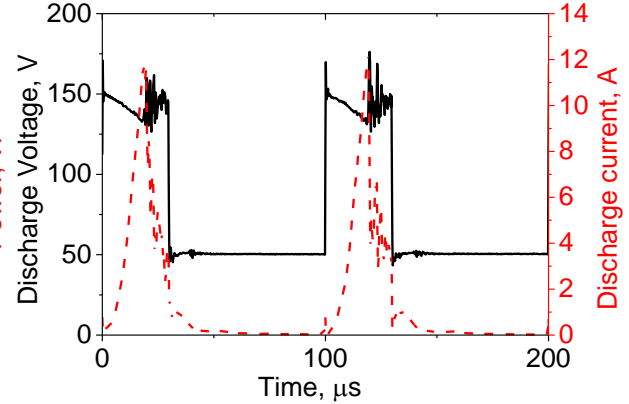


Figure 7. Discharge current trace at $V_0=50V$.

B. Non-smoothing Step-up Chopper Type Power Source

Previous results show that discharge voltage is not necessarily constant. Therefore, as a coordinated PPU, Non-smoothing step-up chopper type circuit is adapted, as shown in Fig. 8. This is almost the same circuit which is often used as a DC-DC converter. The difference is that the output capacitor is relatively small, this makes the output voltage vary under control. This is a turn of 180 degrees concept against conventional PPU concept, the adaption of this circuit has the PPU become the coordinate PPU with the thruster. That is, the characteristic of power source changes with the change of the impedance of the thrusters, if the capacitor and the inductor (reactor) are adequate. When the impedance is low, large pulsed current can be supplied from the reactor (Inductor), and when the impedance is high, the capacitor can keep high discharge voltage for maintaining the discharge.

In this circuit, input voltage, V_{in} , can be bass voltage from the solar cell and output voltage, V_{out} , can be changed by changing the duty ratio of chopping as shown in Equation (2).

$$V_{out} = V_{in} \times \frac{1}{1 - duty} = V_{in} \times \frac{1}{1 - t_{on} \cdot f} \quad (2)$$

Figure 9 shows the discharge current trace, discharge voltage trace and diode current trace at $C=0.5 \mu F$, $V_{out}=250$ V, chopping frequency of 24 kHz, inner coil current of 0.5 A. The red region shows the period that the reactor supply large pulsed current, through a diode and the blue region shows the period that the capacitor supply current and keep high voltage for maintaining the discharge.

Figure 10 shows the discharge current trace for four chopping frequencies, 12 kHz, 16 kHz, 18 kHz and 20 kHz at $C=1 \mu F$ and $V_{out}=150$ V. The thruster (the discharge current) synchronize with the PPU (the discharge voltage) at

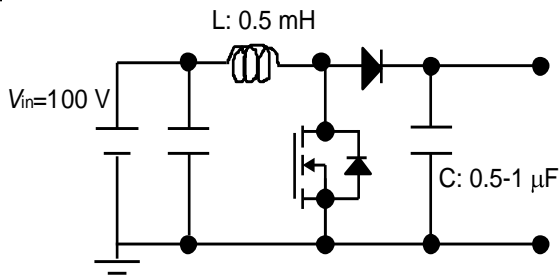


Figure 8. Non-smoothing Step-up Chopper circuit.

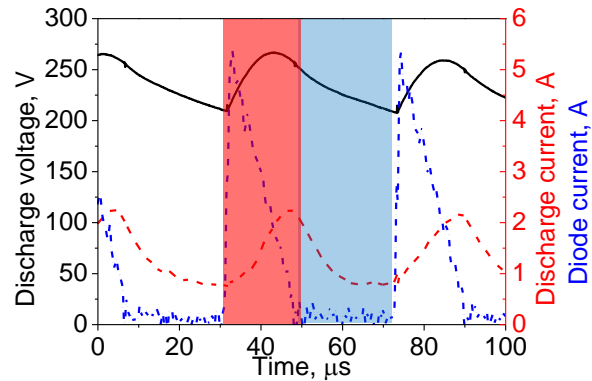


Figure 9. Discharge current, voltage and diode current trace.

16 kHz and 18 kHz. At the condition with chopping frequency of 20 kHz, synchronized period and unsynchronized period coexist. The chopping frequency increase beyond 20 kHz, they defiantly don't synchronize. At low chopping frequency condition, as 12 kHz, the discharge current oscillates at about 2 times larger frequency than the chopping frequency. The point that the discharge current increases and the point that the discharge voltage increases is in coincident, so they may be said "synchronize" but they don't coordinate each other.

Figure 11 shows the thrust and the power consumption on the same condition of Fig.10. The blue regime shows the coordinate operation regime as mentioned above. The thrust and the power consumption decrease with the increase in the chopping frequency. The decrease in the thrust is due to the decrease in the effective discharge voltage as shown in Fig. 10. As the results, the thrust efficiency is almost the constant for various chopping frequencies, from 12 kHz to 21 kHz, as shown in Fig.12. The thrust to power ratio is increased with the increase in the chopping frequency (though the difference is little, the difference is less than the uncertainty). This is due to the decrease in the effective discharge voltage. The thrust efficiency and the thrust to power ratio are 0.24 and 50 mN/kW, respectively. We cannot find the improvement of the thrust performance, since the thrust efficiency and the thrust to power ratio at 150 V constant voltage operation are 0.22 and 50 mN/kW, respectively, considering the effective discharge voltage is higher than 150 V.

Figure 13 shows the thrust and the power consumption at $C=0.5 \mu\text{F}$. The other conditions are the same as Fig.11. The coordinating regime between the thruster and the PPU is expanded, from 12 kHz to 26 kHz. The thrust is almost constant (it changes a little bit but within the uncertainty) compared to Fig.11. The power consumption decreases with the increase in the chopping frequency, and it becomes minimum at frequency of 22 kHz and then it slightly increases. Therefore, the thrust efficiency and the thrust to power ratio increase with the increase in the chopping frequency, as shown in Fig.14. The thrust efficiency and the thrust power ratio are 0.27 and 58 mN/kW, respectively. This result shows the advantage in thrust performance against conventional PPU's(constant voltage operation).

The reason of constant thrust for various chopping frequencies would be due to the effective discharge voltage is constant, as shown in Fig.15. Of course, we should confirm this measuring the ion beam energy distribution function using rerating potential analyzer and among other methods.

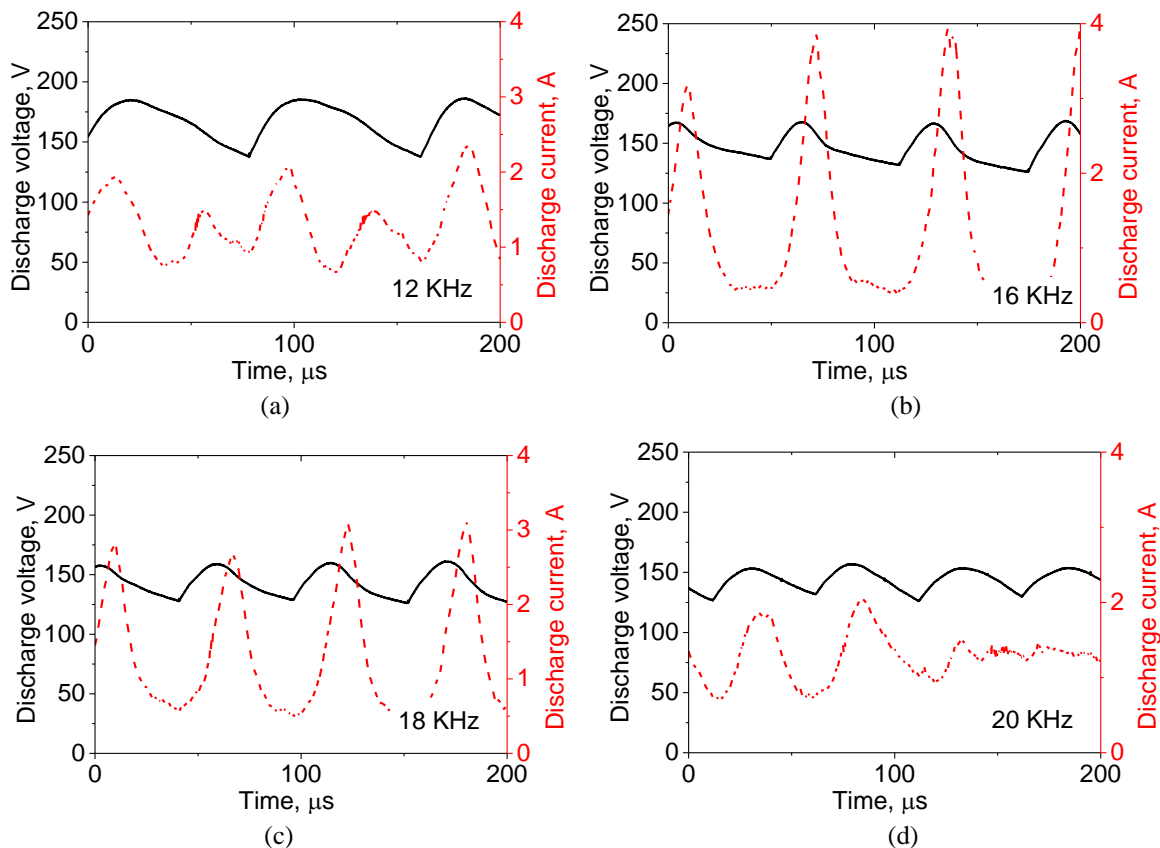


Figure 10. Discharge current trace for various chopping frequencies. (a)12 kHz(b)16 kHz, (c) 18 kHz and (d) 20 kHz

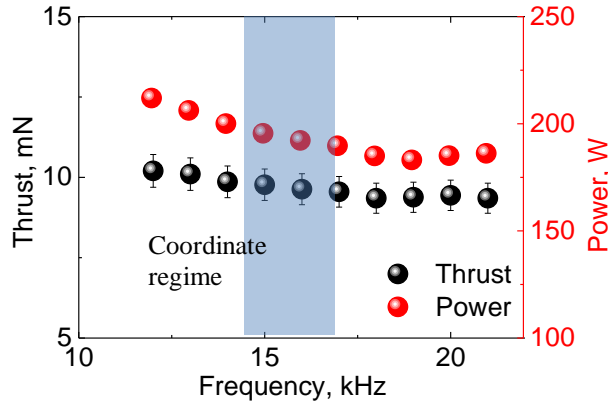


Figure 11. Thrust and power consumption.
 $C=1 \mu\text{F}$ and $V_{\text{out}}=150 \text{ V}$

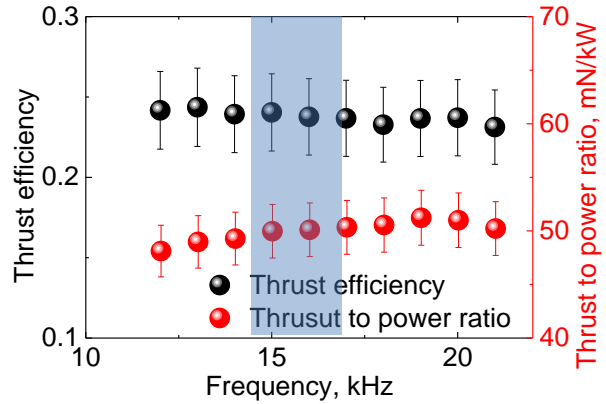


Figure 12. Thrust efficiency and thrust to power ratio.
 $C=1 \mu\text{F}$ and $V_{\text{out}}=150 \text{ V}$

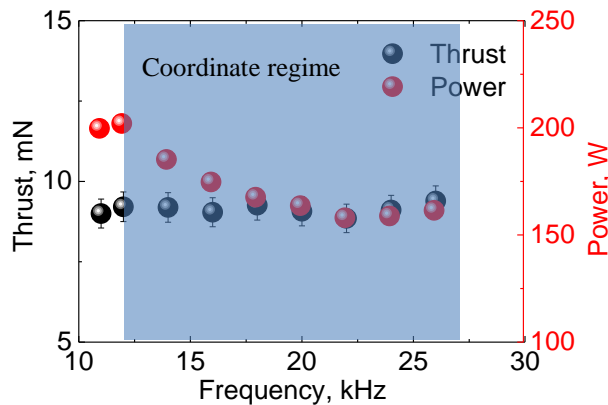


Figure 13. Thrust and power consumption.
 $C=0.5 \mu\text{F}$ and $V_{\text{out}}=150 \text{ V}$

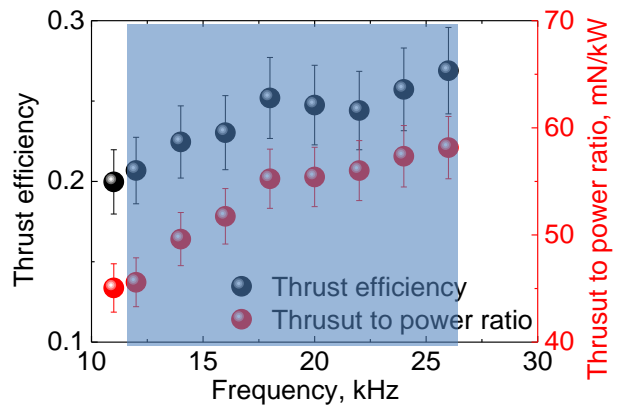


Figure 14. Thrust efficiency and thrust to power ratio.
 $C=0.5 \mu\text{F}$ and $V_{\text{out}}=150 \text{ V}$

The reason that the improvement on the thrust performance using the coordinate PPU against that using a conventional constant voltage power supply would be that the PPU synchronized to the prey-predator oscillation mechanism. That is, a virtuous circle appears, as shown in Fig. 16.

- 1) Plasma density in the ionization zone is low and neutral atoms are fed to the zone. On this period, PPU have the discharge voltage increase but the ionization occurs little because of the low neutral atom density. So the discharge current is low.
- 2) The discharge voltage becomes high and the neutral atom density is enough high to lead effective ionization, so an avalanche of the ionization occurs. As the result, the discharge current increases. The discharge voltage is high, so the potential of the ionization zone is high, that is, the ions gain adequate energy and are propelled from the thruster.
- 3) A starve of neutral atoms leads to the decrease in ionization in the ionization zone. The coordinate PPU decrease discharge voltage simultaneously. Most of the ions have already been accelerated, so there is no influence on the thrust in this regime.
- 4) Back to (1)

PPU varies potential and electron energy coincidentally with the number density of neutral atoms. This allows the thrust not to decrease, since most of the ionization occurs while the space potential in the ionization zone keeps high. And this allows to reduce the power consumption, since the coordinated PPU decreases the discharge voltage while the ionization is little. Therefore, this synchronized cycle contributes the improvement of the thrust performance.

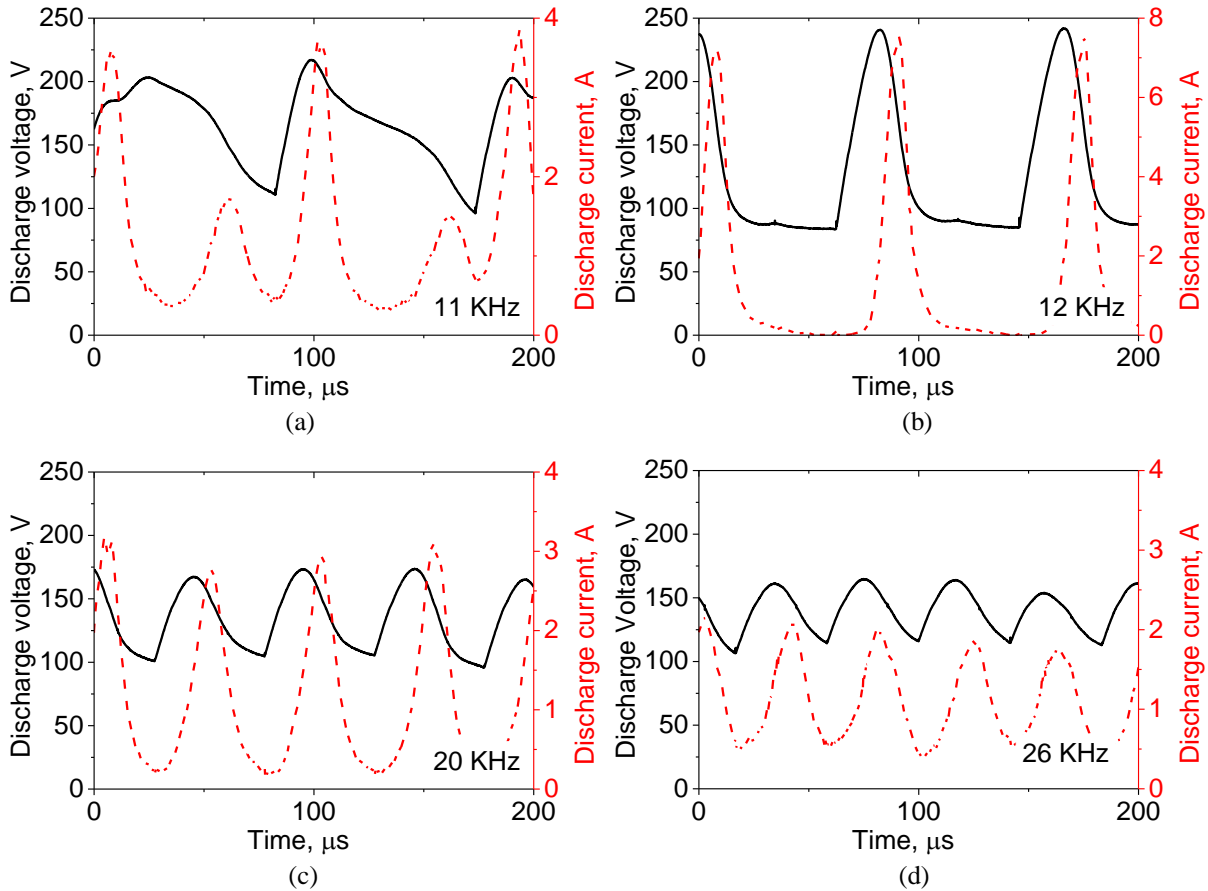


Figure 15. Discharge current trace for various chopping frequencies. (a)11 kHz(b)12 kHz, (c) 20 kHz and (d) 26 kHz

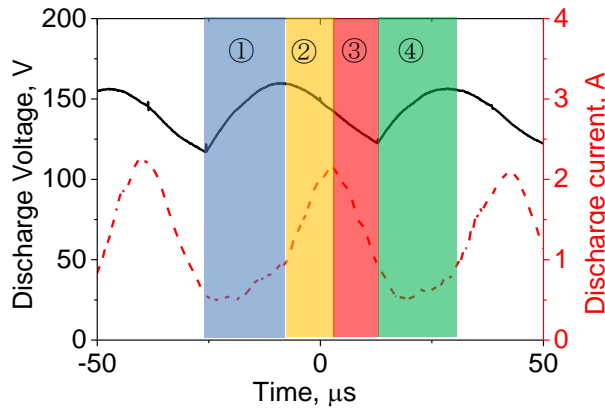


Figure 16. Virtuous circle synchronizing with ionization oscillation.

IV. Conclusion

As a coordinate PPU with Hall thrusters, non-smoothing step-up chopper type PPU has been developed and the thrust performances were investigated using the 1 kW class magnetic layer type Hall thruster developed at Kyushu University. The thrust efficiency and the thrust to power ratio are 0.27 and 58 mN/kW respectively. These are superior to those with 150 V constant voltage operation, 0.22 and 50 mN/kW.

The most advantage of the coordinate PPU is light weigh. Since the capacitor is relatively small compared to the conventional PPU, which is the most massive component in the PPU. It also allows to use the ceramic or film capacitor, this adoption leads to extend the PPU's lifetime.

The coordinate PPU with "Lightweight and small size" and "improvement of the thrust performance" would have a potential to be a mainstream of the Hall thrusters PPU.

Acknowledgments

This work was supported by JSPS KAKENHI Grant Number, 23686123.

References

- ¹Website of Hall thruster research group <http://art.aees.kyushu-u.ac.jp/research/Hall/inspace/inspace.html>
- ² Schönherr, T., Hosoda, M., Cho, S., Koizumi, H., Arakawa, Y., Komurasaki, K. and Yamamoto, N. "Low- cost 20 kW Hall thruster for mass transportation." Asian Joint Conference on Propulsion and Power 2012, Mar. 2012. AJCPP2012-022.
- ³Ito, Y., Nakano, M., Schonherr, T., Cho, S., Komurasaki, K. and Koizumi, H.: In-space transportation of a solar power satellite using a hall thruster propulsion system Renewable Energy Research and Applications (ICRERA), 2012.
- ⁴Nakano, M., Ito, Y. and Komurasaki, K: In-Space Transportation for Solar Power Satellites Using Electric Propulsion, 56th Conference on Space Science and Technology, 2012 (in Japanese).
- ⁵Choueiri, E. Y., "Fundamental difference between the two Hall Thruster Variants," Physics of Plasmas, Vol. 8, No. 11, 2001, pp. 5025–5033.
- ⁶Kaufman, H. R., "Technology of Closed-Drift Thrusters," AIAA Journal, 0001-1452, Vol. 23, No. 1, 1985, pp. 78–87. atistas, G. H., Lin, S., and Kwok, C. K., "Reverse Flow Radius in Vortex Chambers," *AIAA Journal*, Vol. 24, No. 11, 1986, pp. 1872, 1873.
- ⁷Nagano, H. Kajiwara, k., Osuga, H., Ozaki, T., Nakagawa, T. and Shuto, K., "Development status of a New Power Processing Unit of Ion Engine System for the Super Low Altitude Test Satellite", Proceedings of the 31st International Electric Propulsion Conference 2009, Ann Arbor, USA, IEPC2009-9(2009)
- ⁸Choueiri, E., "Plasma oscillations in Hall thrusters," Physics of Plasmas, 8, 4 1411-1426, 2001.
- ⁹Tilinin, G. N., "High-Frequency Plasma Waves in a Hall Accelerator with an Extended Acceleration Zone," Soviet Physics-Technical Physics, Vol. 22, 1977, pp. 974–978.
- ¹⁰ Baranov, V. I., Nazarenko, Yu. S., Petrosov, V. A., Vasin, A.I., and Yashonov, Yu. M. "Theory of Oscillations and Conductivity for Hall Thruster," AIAA Paper 96-3192, July 1996.
- ¹¹ Yamamoto, N., Komurasaki, K., Arakawa, Y. "Discharge Current Oscillation in Hall Thrusters," *J. Propulsion & Power*, Vol.21, (2005) pp.870-876.
- ¹²Boeuf, J. P., and Garrigues, L., "Low Frequency Oscillation in a Stationary Plasma Thruster," *Journal of Applied Physics*, Vol. 84, No. 7, 1998, pp. 3541–3554.
- ¹³ Yamamoto, N., Yokota ,S., Watanabe K., Sasoh, A., Komurasaki, K., Arakawa, Y. "Suppression of Discharge Current Oscillations in a Hall Thruster," *Trans. Jpn. Society for Aeronautical and Space Sciences*, Vol.48 (2005) pp.169-174.
- ¹⁴ Tamida, T., Nakagawa, T., Suga, I. Osuga, H., Ozaki, T., Matsui, K."Determining parameter sets for low-frequency-oscillation-free operation of Hall thruster" *J. Appl. Phys.*, Vol.102, 043304 (2007)